Synthesis and characterization of O3-$Na_3LiFeSbO_6$: a new honeycomb ordered layered oxide

Citation	Schmidt, W., Berthelot, R., Etienne, L., Wattiaux, A., & Subramanian, M. A. (2014). Synthesis and characterization of O3-$Na_3LiFeSbO_6$: A new honeycomb ordered layered oxide. Materials Research Bulletin, 50, 292-296. doi:10.1016/j.materresbull.2013.10.049
DOI	10.1016/j.materresbull.2013.10.049
Publisher	Elsevier
Version	Accepted Manuscript
Terms of Use	http://cdss.library.oregonstate.edu/sa-termsofuse

Synthesis and characterization of O3-$Na_3LiFeSbO_6$: a new honeycomb ordered layered oxide

Whitney Schmidt[a], Romain Berthelot[a], Laetitia Etienne[b], Alain Wattiaux[b], M. A. Subramanian[a]*

[a]*Department of Chemistry, Oregon State University, Corvallis, OR 97331, USA*

[b]*CNRS, Université de Bordeaux, ICMCB, 87 avenue du Dr. A. Schweitzer, 33608, F-Pessac, France*

Abstract:

A new compound $Na_3LiFeSbO_6$ has been synthesized by conventional solid state methods and investigated using X-ray diffraction, DC magnetic susceptibility, ^{57}Fe Mössbauer spectroscopy and optical measurements. This compound crystallizes in a monoclinic unit cell and is related to a family of honeycomb ordered layered oxide materials where Na^+ fills octahedral interlayer sites between $Li_{1/3}Fe_{1/3}Sb_{1/3}O_2$ slabs of edge sharing octahedra. Each SbO_6 octahedron is surrounded by LiO_6 and FeO_6 octahedra creating a honeycomb arrangement within the slabs. Powder X-ray diffraction indicates the presence of stacking faults. This compound exhibits Curie-Weiss behavior at high temperatures and the effective magnetic moment verifies the presence of high spin Fe^{3+}. The ^{57}Fe Mössbauer spectroscopy confirms Fe^{3+} in an octahedral position and indicates disorder in the arrangement of LiO_6 and FeO_6 octahedra in the $Li_{1/3}Fe_{1/3}Sb_{1/3}O_2$ slabs.

Keywords

Layered compounds; Magnetic properties; Optical properties; Mössbauer Spectroscopy; X-ray Diffraction

*Corresponding author: mas.subramanian@oregonstate.edu

1. Introduction

AMO_2 layered oxides are heavily investigated materials because of their remarkable properties such as superconductivity ($Na_xCoO_2{\cdot}yH_2O$)[1,2] and transparent conductivity ($CuAlO_2$).[3] Most notably, $LiCoO_2$ is used as the positive electrode in lithium batteries due to high ionic conductivity and effective charge cycling.[4–6] Compounds in the AMO_2 family are described as having slabs of MO_2 edge sharing octahedra separated by A^+ cations. Depending on the stacking sequence of the slabs, different intercalations sites for A^+ are available, *i.e.* trigonal prismatic (P), octahedral (O) or linear as in the delafossite structure.[7]

Many studies have focused on substituting 1/3 of the M cations with another X cation resulting in a new family of layered oxides $A_xM_{2/3}X_{1/3}O_2$ with a honeycomb ordering in the $M_{2/3}X_{1/3}O_2$ octahedral slabs, as shown in the top image of Figure 1. In the cases where M is a 2+ cation, the X cation is highly charged (5+ or 6+) depending on the A content (x). The honeycomb order arises because the highly charged X cations prefer greater separation following Pauling's rules for edge sharing octahedra.[8] A few examples of compounds that contain the honeycomb ordering in a layered structure are $A_3M_2XO_6$ (A = Na, Li, Ag, Cu; M = Co, Cu, Mg, Ni, Zn; X = Sb, Bi) and $Na_2M_2TeO_6$ (M = Co, Cu, Mg, Ni, Zn).[9–18] For the $A_3M_2XO_6$ family where the A^+ cations are in octahedral coordination within the interlayer space the adopted structure is labeled as O3 which requires three layers to describe the hexagonal unit cell.[7] The XRD patterns of O3 compounds are commonly indexed to one of three space groups, $P3_112$, $C\,2/m$ or $C\,2/c$. Bréger *et al.* applied first principles calculations for each stacking variant in Li_2MnO_3, *i.e.* $Li_3LiMn_2O_6$, and found that all stacking variations have very close energies with the monoclinic space groups only having a 2 meV difference.[19] Since there are

multiple stacking sequences available for these layered materials, stacking faults, or a disruption in the layering sequence, are common. For the $Na_2M_2TeO_6$ compounds, three structures are known with the space groups $P6_322$ (M = Co, Mg, Zn), $P6_3/mcm$ (M = Ni) and $C2/m$ (M = Cu).[13,20] Excluding $Na_2Cu_2TeO_6$, these materials are known as P2 structures where the interlayer sites are partially filled by Na^+ ions and two layers are required to describe the hexagonal unit cell. Due to the partial filling and coordination of the interlayer sites, larger windows are available for fast ionic conduction[13] leading to a recent study by Gupta *et al.* who investigated $Na_{2-x}M_2TeO_6$ (M = Co, Ni) as electrode materials for Na ion batteries.[21]

Honeycomb ordered layered oxides are a growing family of compounds with many new compositions being reported. Zvereva *et al.* discovered Li_4FeSbO_6, where the $Li_{1/3}Fe_{1/3}Sb_{1/3}O_2$ slabs are mostly ordered in a honeycomb fashion isolating the SbO_6 octahedra from one another.[22] Also, Kumar *et al.* has synthesized and characterized many new layered compositions of $Li_8M_2Te_2O_{12}$ (M^{2+} = Co, Cu, Ni, Zn) and $Li_8M_2Sb_2O_{12}$ (M^{3+} = Al, Cr, Fe, Ga).[23] Another study into the heterovalent substitutions for M within the $Na_2M_2TeO_6$ layered oxides; Nalbandyan *et al.* discovered one new compound, $Na_2LiFeTeO_6$. These authors also investigated $Na_2NiMSbO_6$ (M = Al, Fe) but did not find a new honeycomb layered oxide.[24] Thus far the only successful report of heterovalent substitutions in the $Na_3M_2SbO_6$ family was by Politaev *et al*. who investigated the ternary phase diagram for Na_2O – Fe_2O_3 – Sb_2O_z and discovered Na_4FeSbO_6, a composition potentially related to the honeycomb layered structures. These authors also investigated the Ag exchange product and determined a composition of $Ag_3NaFeSbO_6$.[25]

In this paper we report on the synthesis and characterization of a new compound in the honeycomb ordered layered oxide family, O3-$Na_3LiFeSbO_6$.

2. Experimental

Polycrystalline powder samples of $Na_3LiFeSbO_6$ and Na_4FeSbO_6 were prepared by solid state synthesis techniques. Sodium carbonate (Na_2CO_3, Spectrum Chemical 99.5%), antimony oxide (Sb_2O_3, J. T. Baker high purity) and lithium carbonate (Li_2CO_3, Aldrich 99.6%) were thoroughly ground together in the desired stoichiometric proportions. The sodium carbonate and lithium carbonate were dried at 120 °C prior to weighing to prevent moisture contamination. The pelletized samples were loaded into an alumina boat and heated for 48 hrs at 1000 °C (ramp rate of 5 °C min^{-1}) with one intermediate grinding. After the heat treatment, the furnace was allowed to cool to room temperature before removal of the samples.

Powder X-ray diffraction (PXRD) measurements were carried out on a Rigaku Miniflex II diffractometer using Cu Kα radiation and a graphite monochromator on the diffracted beam. The powder samples were loaded on an oriented Si single crystal zero background sample holder (MTI corp.). Measurements were collected from 10° to 80° 2θ (steps of 0.02°) with a 2 s fixed time. Le Bail lattice refinement with *C* 2/c space group was performed with the GSAS software equipped with the EXPGUI suite.[26,27]

Chemical composition was determined by Inductively Coupled Plasma Atomic Emission Spectroscopy (ICP-AES) on a Varian 720 ES. Powder samples (~ 10 mg) were dissolved into a dilute nitric acid solution heated at 70 °C under constant stirring.

Zero field cooled (ZFC) DC magnetization data were collected with a Quantum Design Physical Property Measurement System (PPMS) using the ACMS mode. Measurements were collected from 5 to 300 K under a 0.5 T magnetic field.

In order to evaluate Fe^{3+} local environments of the studied ferrite compounds, ^{57}Fe Mössbauer spectra were collected at 293 K. Both analyses are in transmission mode and were obtained with a conventional constant acceleration spectrometer (HALDER) with rhodium matrix source. As the samples contain about 10 mg natural iron per cm^3, the line broadening due to thickness of samples can be neglected. The spectra refinement was performed in two steps. First, the fitting of Mössbauer patterns as a series of Lorentzian profile peaks allowed the calculation of position (δ), amplitude and width (Γ) of each peak: thus, experimental hyperfine parameters were determined for the various iron sites. Second, spectra analysis was made in terms of quadrupolar splitting distribution P(Δ) with the Hesse and Rubartsch method [28]; Γ and δ were fixed at values determined in the first refinement. This method, which was used because of the line broadening notably observed, leads to a peak shape different from a Lorentzian profile which is characteristic of disordered compounds with a site distribution.

Diffuse reflectance measurements were carried out on packed powder samples with a halogen source (200 – 1150 nm) passed through bifurcated fiber optic wire and magnesium oxide (MgO, Sigma Aldrich, 99.9%) as the white reference. The data was collected by the bifurcated optic cable and carried to an Ocean Optics HR4000 spectrophotometer. The collected data was converted to absorbance using the Kubelka-Munk relation.[29]

3. Results and Discussion

3.1: X-ray Diffraction

The powder X-ray diffraction pattern (PXRD) of $Na_3LiFeSbO_6$ indicates a single phase compound indexed to the monoclinic *C* 2/*c* space group (Figure 2), which is related to the $A_3M_2XO_6$ layered honeycomb ordered oxides. The chemical composition was analyzed by ICP-AES which confirmed $Na_3LiFeSbO_6$ with Na/Li = 3.00(5) as well as both Li/Fe and Fe/Sb close to 1. Lattice refinement using the Le Bail method gives the lattice parameters *a* = 5.3274(2) Å, *b* = 9.2049(2) Å, *c* = 11.377(3) Å and β = 108.47(1)°. The 18 – 33° 2θ reflections have a high sloping background, highlighted in the inset of Figure 2, indicative of a large degree of disorder and stacking faults within the layered structure. This PXRD pattern is similar to that of Na_4FeSbO_6 reported by Politaev *et al*.; however, they indexed the pattern to $P2_112$ space group which resulted in a mismatch of some super lattice reflections.[25] We have successfully indexed this compound to the *C* 2/*c* space group with lattice parameters *a* = 5.4191(2) Å, *b* = 9.3977(2) Å, *c* = 11.530(3) Å and β = 108.35(1)°. The increase in lattice parameters for Na_4FeSbO_6 compared to $Na_3LiFeSbO_6$ is in good agreement with the difference in ionic radii of Na^+ (1.02 Å) and Li^+ (0.76 Å).[30]

Although a complete structural analysis is difficult for disordered materials, this compound can be related to the honeycomb layered oxide materials. The slab ordering and monoclinic structure of $Na_3LiFeSbO_6$ are shown in the upper and lower images of Figure 1. The $LiFeSbO_6$ slabs are ordered in such a way that the SbO_6 octahedra are separated from one another according to Pauling's rules for edge sharing octahedra.[8] The honeycomb pattern around the SbO_6 is a disordered arrangement of Li and Fe indicated in the top image of Figure 1. This disorder is further investigated by ^{57}Fe Mössbauer spectroscopy to be discussed later. The slabs are separated by the Na^+ ions located in octahedral positions between the slabs.

In our attempt to study the solid solution of Na_4FeSbO_6 and Li_4FeSbO_6, only $Na_3LiFeSbO_6$ was formed phase pure, whereas the other intermediate compounds $Na_2Li_2FeSbO_6$ and $Li_3NaFeSbO_6$ resulted in two phase products made up of the parent compounds. These hypothetical compositions could result in two situations: a mixing of both Li^+ and Na^+ in the interslab space and in the slabs or Li^+ filling the interslab space while Na^+ occupies an octahedral position in the slabs. Such a configuration would be difficult when considering the large difference in the ionic radii of Li^+ (0.76 Å) and Na^+ (1.02 Å) in the 6-fold coordination.[30,31] Although Li^+ is slightly larger than the Fe^{3+} (H.S. 0.645 Å) and Sb^{5+} (0.60 Å) it is more likely that it will sit within the slabs and Na^+ will fill the interslab space which helps stabilize $Na_3LiFeSbO_6$ and prevents the other compositions from forming.[30]

3.2: Magnetic Susceptibility

The ZFC DC magnetic susceptibility (χ_m) and inverse susceptibility ($1/\chi_m$) vs. temperature curves for $Na_3LiFeSbO_6$ and $Na_3NaFeSbO_6$ are shown in Figure 3 (left and right, respectively). The Curie-Weiss fit for $Na_3LiFeSbO_6$ from 150 – 300 K resulted in an effective moment of 5.84 μ_B which agrees with the spin-only theoretical moment of one Fe^{3+} (S = 5/2, $\mu_{theor.}$ = 5.92 μ_B). The negative Weiss constant (θ = -7.90 K) indicates the presence of antiferromagnetic short range interactions, although long range ordering is not detected for this compound down to 5 K in contrast to a reported antiferromagnetic transition at T_N = 3.6 K in $Li_3LiFeSbO_6$.[22] This lack of long range order indicates disorder in the FeO_6 arrangement preventing any long range or superexchange interactions. For comparison, the magnetic susceptibility of $Na_3NaFeSbO_6$ is provided and the Curie-Weiss fit resulted in a μ_{eff} = 5.73 μ_B. This again is in good agreement with the spin-only contributions for high spin Fe^{3+}. Long range ordering was not observed

above 5 K and the positive Weiss constant (θ = 3.70 K) indicates short range weak ferromagnetic interactions.

3.3: Mössbauer Spectroscopy

The ^{57}Fe Mössbauer spectrum for $Na_3LiFeSbO_6$ measured at room temperature indicates one paramagnetic doublet, Figure 4. Upon initial fitting of the data assuming a Lorentzian profile, the obtained Mössbauer parameters were δ = 0.343 mm/s, Γ = 0.33 mm/s and Δ = 0.53 mm/s. The isomer shift (δ) is characteristic for high-spin Fe^{3+} in an octahedral position. Thus, this preliminary fit using Lorentzian profile lines allowed the characterization of one doublet assigned to an iron that is in accordance with the expected crystallographic site. Nevertheless, the calculation led to a slightly larger value of linewidth compared to the value of the experimental width (Γ_{exp} = 0.25 mm/s) suggesting the existence of quadrupolar splitting distribution which may be associated to a local cationic disorder around the Fe nucleus. Thus, a second computation allowed the analysis of spectra in terms of quadrupolar splitting distribution.[28] For this calculation, the half-height width Γ was fixed at 0.25 mm/s and the isomer shift was fixed at the value determined in the first treatment. The result of the refinement is shown in Figure 4. The average quadrupolar splitting determined by the second fitting is Δ = 0.59 mm/s and the width of this distribution confirms the existence of a cationic disorder around Fe. This is in agreement with the disorder evidenced in the PXRD pattern. The value of mean quadrupolar splitting is somewhat high indicating a slight deformation of the FeO_6 octahedron resulting from the difference in ionic radii of its neighbors Li^+ and Sb^{5+}.

3.4: Optical Characterization

Diffuse reflectance measurements were carried out on $Na_3LiFeSbO_6$ and Na_4FeSbO_6 compositions, both of which are a light shade of orange when finely ground. The diffuse reflectance data was transformed to absorbance using the Kubelka-Munk relation.[29] Figure 5 shows the absorbance vs. eV spectra for the two compositions. The band gaps were estimated by extrapolating the absorption onset to the x-axis. The resulting band gaps were 3.19 eV and 3.18 eV for $Na_3LiFeSbO_6$ and Na_4FeSbO_6, respectively.

4. Conclusions

In our search for compounds in the Na_4FeSbO_6 – Li_4FeSbO_6 system, a new composition $Na_3LiFeSbO_6$ was successfully obtained by solid state reaction. This layered oxide is characterized by a honeycomb ordering within the slab with each SbO_6 octahedron surrounded by LiO_6 and FeO_6 octahedra. This compound appears to be the only composition that forms between Na_4FeSbO_6 and Li_4FeSbO_6 as it is not possible to have Li^+ and Na^+ simultaneously in the interslab space. The monoclinic cell seems to be the best index for the XRD pattern; however, the presence of stacking faults may alter the fit and prevent a full refinement of the structure. This compound exhibits an effective magnetic moment in agreement with high spin Fe^{3+} assuming spin-only contributions. Long range magnetic ordering is not observed, as was not expected due to the high degree of disorder in this compound. ^{57}Fe Mössbauer spectroscopy indicates a cationic disorder around Fe verifying a random arrangement of Li and Fe in the honeycomb lattice.

Acknowledgements

This work has been supported by NSF grant DMR 0804167.

References

[1] K. Takada, H. Sakurai, E. Takayama-Muromachi, F. Izumi, R.A. Dilanian, T. Sasaki, Nature 422 (2003) 53.

[2] R.E. Schaak, T. Klimczuk, M.L. Foo, R.J. Cava, Nature 424 (2003) 527.

[3] H. Kawazoe, M. Yasukawa, H. Hyodo, M. Kurita, H. Yanagi, H. Hosono, Nature 389 (1997) 939.

[4] K. Mizushima, P.C. Jones, P.J. Wiseman, J.B. Goodenough, Mater. Res. Bull. 15 (1980) 783.

[5] J.-M. Tarascon, M. Armand, Nature 414 (2001) 359.

[6] M. Armand, J.-M. Tarascon, Nature 451 (2008) 652.

[7] C. Delmas, C. Fouassier, P. Hagenmuller, Phys. BC 99 (1980) 81.

[8] L. Pauling, J. Am. Chem. Soc. 51 (1929) 1010.

[9] C. Greaves, S.M.A. Katib, Mater. Res. Bull. 25 (1990) 1175.

[10] R. Nagarajan, S. Uma, M.K. Jayaraj, J. Tate, A.W. Sleight, Solid State Sci. 4 (2002) 787.

[11] O.A. Smirnova, V.B. Nalbandyan, A.A. Petrenko, M. Avdeev, J. Solid State Chem. 178 (2005) 1165.

[12] V.V. Politaev, V.B. Nalbandyan, A.A. Petrenko, I.L. Shukaev, V.A. Volotchaev, B.S. Medvedev, J. Solid State Chem. 183 (2010) 684.

[13] M.A. Evstigneeva, V.B. Nalbandyan, A.A. Petrenko, B.S. Medvedev, A.A. Kataev, Chem. Mater. 23 (2011) 1174.

[14] E. Climent-Pascual, P. Norby, N.H. Andersen, P.W. Stephens, H.W. Zandbergen, J. Larsen, R.J. Cava, Inorg. Chem. 51 (2011) 557.

[15] R. Berthelot, W. Schmidt, S. Muir, J. Eilertsen, L. Etienne, A.W. Sleight, M.A. Subramanian, Inorg. Chem. 51 (2012) 5377.

[16] R. Berthelot, W. Schmidt, A.W. Sleight, M.A. Subramanian, J. Solid State Chem. 196 (2012) 225.

[17] J.H. Roudebush, N.H. Andersen, R. Ramlau, V.O. Garlea, R. Toft-Petersen, P. Norby, R. Schneider, J.N. Hay, R.J. Cava, Inorg. Chem. (2013).

[18] W. Schmidt, R. Berthelot, A.W. Sleight, M.A. Subramanian, J. Solid State Chem. 201 (2013) 178.

[19] J. Bréger, M. Jiang, N. Dupré, Y.S. Meng, Y. Shao-Horn, G. Ceder, C.P. Grey, J. Solid State Chem. 178 (2005) 2575.

[20] J. Xu, A. Assoud, N. Soheilnia, S. Derakhshan, H.L. Cuthbert, J.E. Greedan, M.H. Whangbo, H. Kleinke, Inorg. Chem. 44 (2005) 5042.

[21] A. Gupta, C. Buddie Mullins, J.B. Goodenough, J. Power Sources 243 (2013) 817.

[22] E.A. Zvereva, O.A. Savelieva, Y.D. Titov, M.A. Evstigneeva, V.B. Nalbandyan, C.N. Kao, J.-Y. Lin, I.A. Presniakov, A.V. Sobolev, S.A. Ibragimov, M. Abdel-Hafiez, Y. Krupskaya, C. Jähne, G. Tan, R. Klingeler, B. Büchner, A.N. Vasiliev, Dalton Trans. 42 (2013) 1550.

[23] V. Kumar, N. Bhardwaj, N. Tomar, V. Thakral, S. Uma, Inorg. Chem. 51 (2012) 10471.

[24] V.B. Nalbandyan, A.A. Petrenko, M.A. Evstigneeva, Solid State Ionics 233 (2013) 7.

[25] V.V. Politaev, V.B. Nalbandyan, Solid State Sci. 11 (2009) 144.

[26] A.C. Larson, R.B. Von Dreele, Los Alamos Natl. Lab. Rep. LAUR 86-748 (1994).

[27] B.H. Toby, J. Appl. Crystallogr. 34 (2001) 210.

[28] J. Hesse, A. Rubartsch, J. Phys. [E] 7 (1974) 526.

[29] P. Kubelka, F. Munk,, Z. Tech. Phys. 12 (1931) 593.

[30] R.D. Shannon, Acta Crystallogr. Sect. 32 (1976) 751.

[31] W.C. Sheets, E.S. Stampler, M.I. Bertoni, M. Sasaki, T.J. Marks, T.O. Mason, K.R. Poeppelmeier, Inorg. Chem. 47 (2008) 2696.

Figure Captions

Figure 1. Ideal honeycomb arrangement within the slabs of $AM_{2/3}X_{1/3}O_2$ materials. Top image illustrates possible disorder in the honeycomb arrangement in the quaternary layered oxide materials. The bottom image shows the monoclinic cell with the octahedral interlayer sites filled by Na ions.

Figure 2. Experimental PXRD pattern of $Na_3LiFeSbO_6$ (experimental, calculated and difference profiles respectively as black, red and purple lines; Bragg positions shown with blue ticks). The large sloping background from 18 to 33° 2θ (highlighted in the inset) indicates there are stacking faults and a high degree of disorder in the structure.

Figure 3. Magnetic susceptibility vs. temperature plots with inset plot of inverse magnetic susceptibility vs. temperature. The high temperature region 150 – 300 K was fit using the Curie-Weiss law $\chi_m = C/(T-\theta)$.

Figure 4. ^{57}Fe Mössbauer spectra for $Na_3LiFeSbO_6$ (black dotted line) and the calculated fit (blue solid line).

Figure 5. Diffuse reflectance measurement transformed to absorbance vs. eV for powder samples $Na_3LiFeSbO_6$ and $Na_3NaFeSbO_6$. The band gaps were estimated by extrapolating the x-intercept from the absorption onset.

Figure 1.

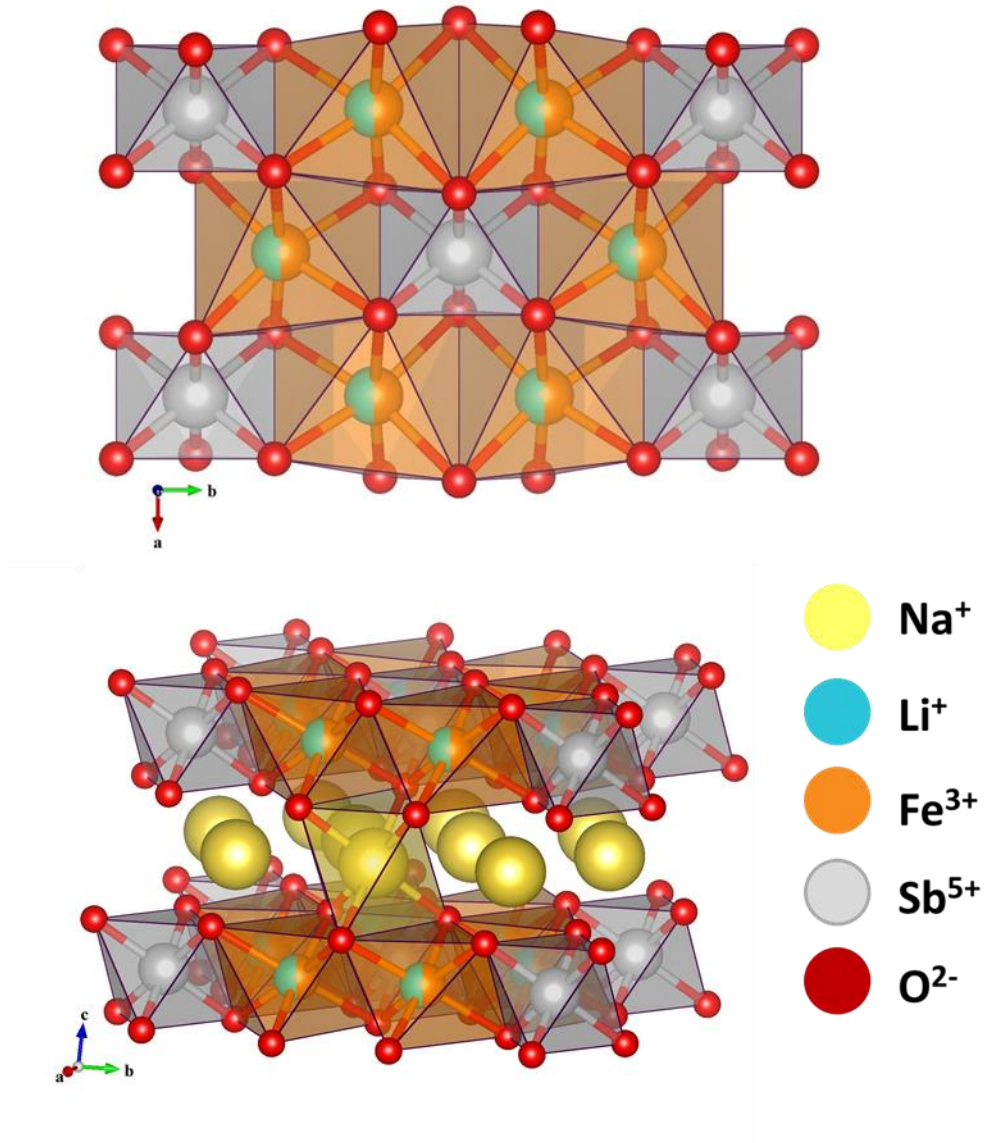

Figure 2.

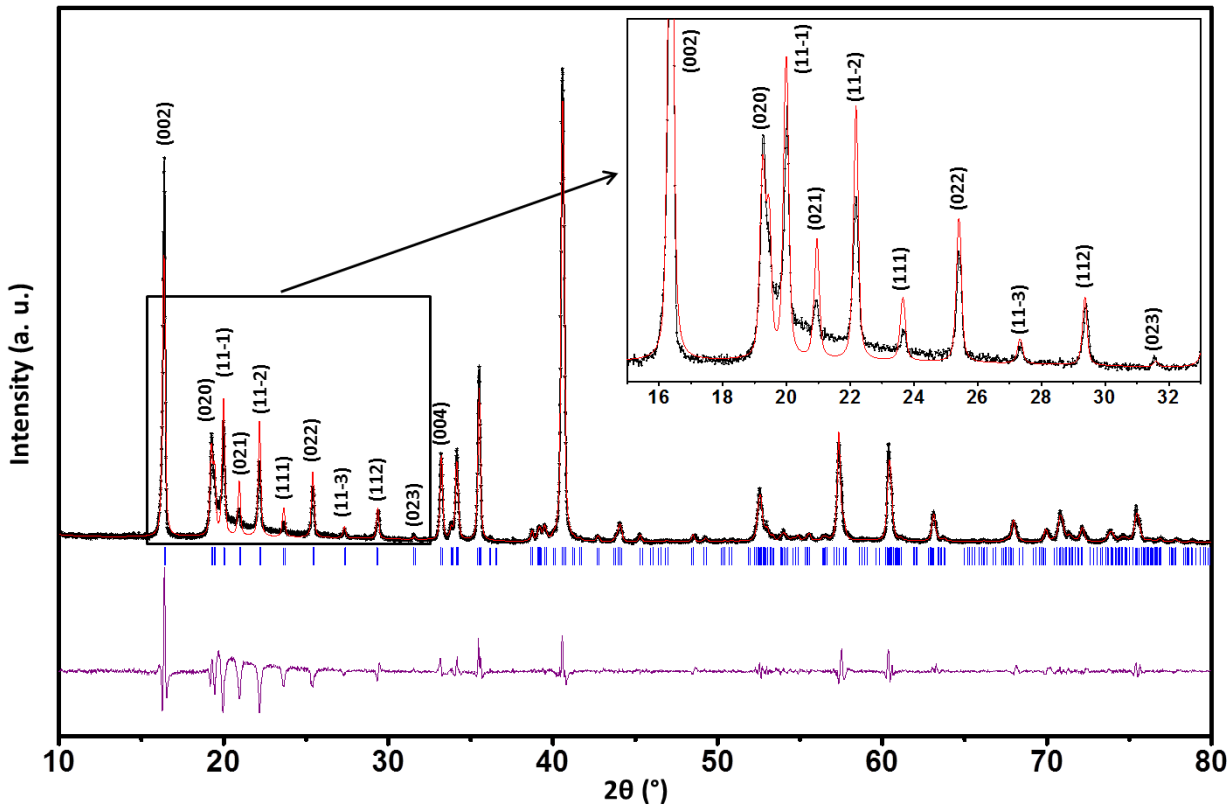

Figure 3.

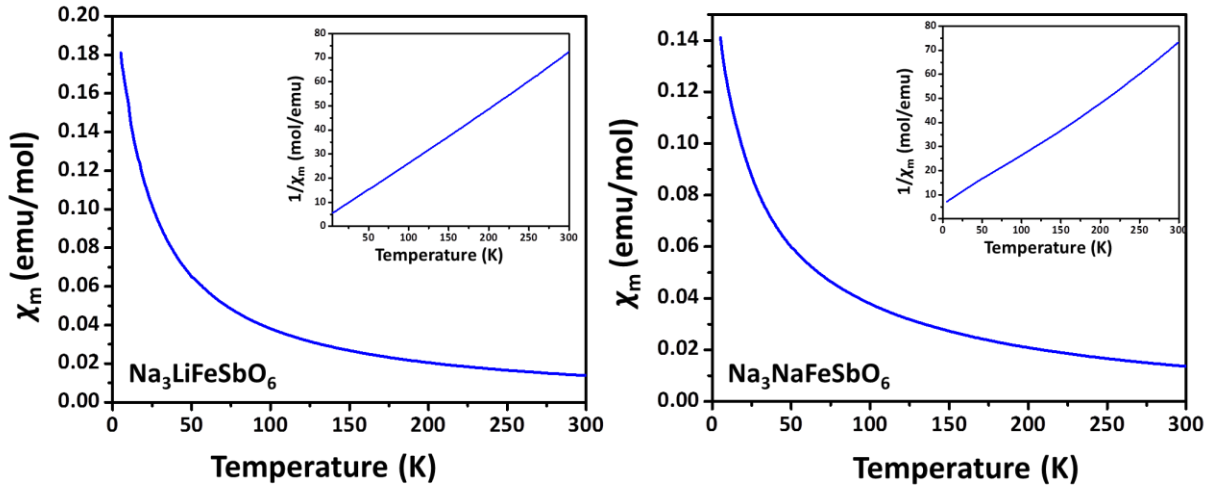
χ_m (emu/mol)
Temperature (K)
$Na_3LiFeSbO_6$
$1/\chi_m$ (mol/emu)
Temperature (K)
$Na_3NaFeSbO_6$

Figure 4.

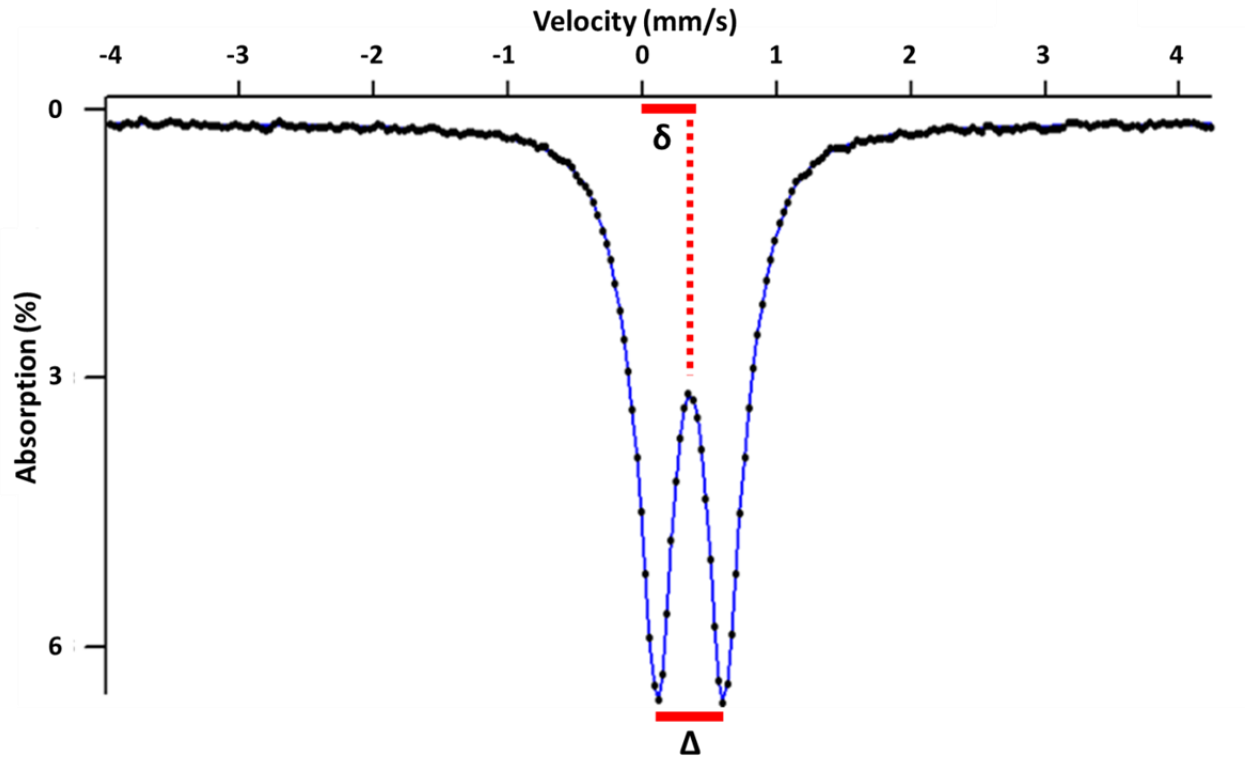

Figure 5.

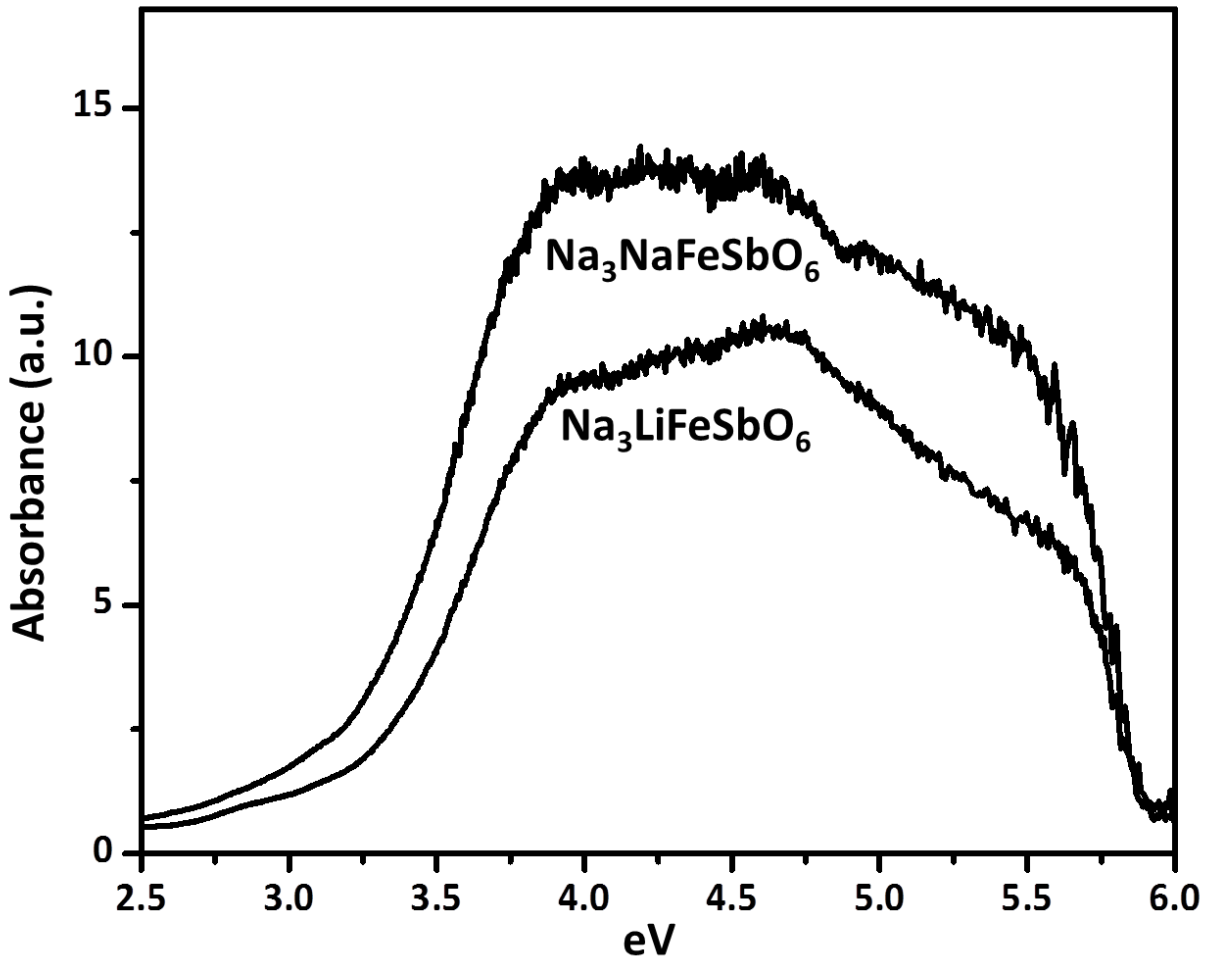
Absorbance (a.u.)
15
10
5
0
2.5
3.0
3.5
4.0
4.5
5.0
5.5
6.0
eV
Na3NaFeSbO6
Na3LiFeSbO6